



Photoluminescence studies on rare earth titanates prepared by self-propagating high temperature synthesis method

Lyjo K. Joseph^{a,*}, K.R. Dayas^{b,c}, Soniya Damodar^b, Bindu Krishnan^{a,b,1}, K. Krishnankutty^c, V.P.N. Nampoori^a, P. Radhakrishnan^a

^a International School of Photonics, Cochin University of Science and Technology, Kalamssery, Kochi 682022, Kerala, India

^b Centre for Materials for Electronics Technology, Athani PO, Thrissur 680771, Kerala, India

^c Department of Chemistry, University of Calicut, Calicut University PO, Tenhipalam, Malappuram 673635, Kerala, India

ARTICLE INFO

Article history:

Received 11 January 2008

Received in revised form 29 February 2008

Accepted 19 March 2008

PACS:

78.55.-m

78.55.Mb

Keywords:

Photoluminescence

Rare earth titanates

Self-propagating high temperature

synthesis

Pyrochlore

ABSTRACT

The laser-induced luminescence studies of the rare earth titanates ($R_2Ti_2O_7$) ($R = La, Nd$ and Gd) using 355 nm radiation from an Nd:YAG laser are presented. These samples with submicron or nanometer size are prepared by the self-propagating high temperature synthesis (SHS) method and there is no known fluorescence shown by these rare earths in the visible region. Hence, the luminescence transitions shown by the $La_2Ti_2O_7$ near 610 nm and $Gd_2Ti_2O_7$ near 767 nm are quite interesting. Though La^{3+} ions with no 4f electrons have no electronic energy levels that can induce excitation and luminescence processes in the visible region, the presence of the Ti^{3+} ions leads to luminescence in this region.

© 2008 Elsevier B.V. All rights reserved.

1. Introduction

Rare earth titanates ($R_2Ti_2O_7$) (RET) have interesting dielectric, piezoelectric and ferroelectric properties [1–3]. These materials usually possess a cubic pyrochlore structure [4–7] for the ions with small R^{3+} (Sm^{3+} – Lu^{3+}), while with the larger R^{3+} (La^{3+} – Nd^{3+}) exhibit a monoclinic structure [2,8]. Pyrochlore RETs and zirconates find numerous applications such as hosts for fluorescence centres, high temperature pigments, catalysts, thermal barrier coatings, ionic/electronic conductors, host phase in nuclear waste control, etc. [3,9–11]. Some of the pyrochlores exhibit good catalytic activity, high melting point, low thermal conductivity, high thermal and phase stability, which make them promising for the catalytic combustion applications and thermal barrier coatings [12,13].

Photoluminescence (PL) is a non-destructive and highly sensitive method commonly used to study the photo-physical and

photochemical properties in the photo assisted reactions. It is closely related to the surface stoichiometry and the nature of surface states, which can usually be changed by the annealing process [14]. Investigations have shown that the luminescence efficiency of materials can be improved by appropriate impurity addition [15,16].

The rare-earth (RE) doped laser crystals, glasses and ceramics, which possess trivalent RE ions, are popular solid-state gain media. RE ions are also used as co-dopants for quenching the population in certain energy levels by the energy transfer processes, or for realizing saturable absorbers, or as optically passive constituents of laser crystals [17]. The PL and decay times in nano-structured xerogel and annealed sol–gel silica glasses doped with RE ions, transition metal ions, metal complexes and semiconductor nano-crystals are investigated previously to study the excitation energy transfer processes, which reflect the optical properties of these confined nano-porous networks [18–20]. RE metal compounds, especially their oxides, have become of increasing interest in recent years because of their special PL and catalytic properties [21,22]. RE-based phosphors play a critical and indispensable role as luminescent materials in the display industry. Synthesize of high quality RE-based phosphors materials in the nano-region is thus important. With the growing

* Corresponding author. Tel.: +91 484 2575848; fax: +91 484 2576714.

E-mail addresses: lyjokjoseph@yahoo.co.in, lyjo@cusat.ac.in (L.K. Joseph).

¹ Present address: Indian Institute of Space Science and Technology, VSSC Campus, Thiruvananthapuram, Kerala, India.

interest in nanoscale RE activated phosphors for display applications, many efforts have been made to develop these nanoscale phosphor materials because of their good luminescence characteristics, stability in high vacuum, and absence of corrosive gas emission under electron bombardment [23,24].

The RETs are prepared by self-propagating high temperature synthesis (SHS) method, which is also known as the self-ignition synthesis or combustion synthesis. The titanates and oxides prepared by SHS method are superior to those prepared by conventional methods. The salient feature of SHS method is that it utilizes reaction heat, instead of electric power. The SHS products are good quality submicron or nanometre sized powders with non-agglomerated nature. It can be synthesized to phase pure and sintered to high density at relatively lower temperatures [25–29].

2. Sample preparation

The corresponding RE oxides (0.02 mol) are dissolved in hot HNO_3 . This solution is slowly heated on a boiling water bath to remove the excess acid, if any, and evaporated to get the dry RE nitrate. To this, TiO_2 (0.04 mol) and urea (0.16 mol) are added and slowly heated on an electric Bunsen and the contents in the beaker are thoroughly mixed by stirring. Urea acts as the solid fuel in the reaction and its molar ratio is very crucial. As the temperature increases to around 300°C , urea melts and starts decomposing with the evolution of ammonia. When the temperature reaches $\sim 350^\circ\text{C}$, copious brown fumes of oxides of nitrogen start evolving. At this stage a spontaneous incandescent reaction takes place vigorously and the mixture self-ignites at about 400°C along with evolution of large amount of gases. The content of the vessel froths up to a highly porous network of foam like structure, which almost fills the reaction vessel and gradually the flame subsides. The highly porous network of the fine crystallites of the RET formed is cooled to room temperature. The powder is calcined, pelletised and sintered at $1350\text{--}1550^\circ\text{C}$.

3. Experimental details

The relative reflectance spectra of the pelletised samples are taken using a JASCO V-570 UV/VIS/NIR spectrophotometer with the model SLM-468 single reflection attachment at an angle of incidence approximately 5° with aluminium-deposited plane mirror as reference. The surface area of the samples is measured using the Quanta chrome Nova model 1200 BET analyzer and from the data on density of the SHS powders, their average particle size can be calculated (Table 1). The Bruker AXS 5005 XRD machine with $\text{Cu K}\alpha$ ($\lambda = 1.5418 \text{ \AA}$) radiation is used for evaluating the products synthesized in this study. The SEM microstructure measurements are done using a JEOL JSM-840A SEM.

Using the pellets sintered at 1350°C the luminescence studies are carried out at room temperature with the third harmonic of an Nd:YAG laser (355 nm, 7 ns Spectra Physics Quanta Ray). The luminescence spectrum is recorded using 0.5 m triple grating spectrograph/monochromator assembly (Spectrapro 500i Acton Research) attached with a CCD camera (Roper Scientific NTE/CCD 1340/100-EM).

Table 1
Details of the RET samples used for the study

$\text{R}_2\text{Ti}_2\text{O}_7$ (R=)	Density (g/cm^3)	Surface area (m^2/g)	Average particle size (nm)
Gd	6.56	13.67	67
La	5.78	11.40	91
Nd	6.11	16.01	61

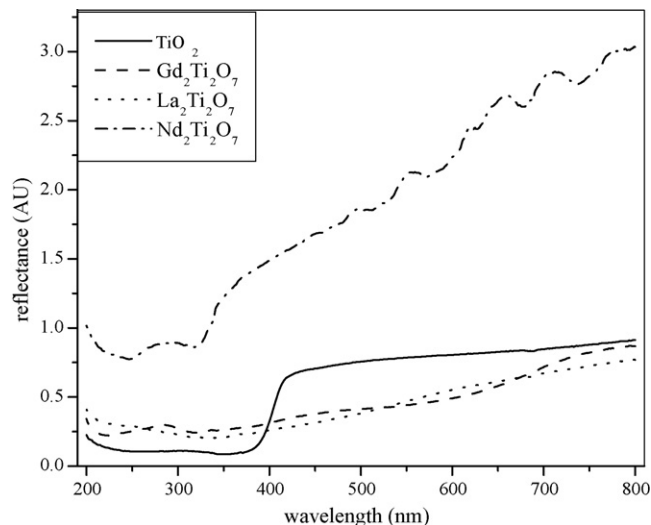


Fig. 1. Reflectance spectra of the samples.

4. Results and discussion

From the reflectance spectrum, shown in Fig. 1, it is clear that the samples have absorption at around 355 nm.

The XRD of these SHS powders show the amorphous or microcrystalline nature of the products. However, the crystallinity gradually improves on calcination at different temperatures and at 1200°C , transforms to 100% phase pure crystalline material. The peaks in the spectra of $\text{R}_2\text{Ti}_2\text{O}_7$ synthesized by SHS-urea method and calcined at 1200°C (Fig. 2), where R=La and Nd match exactly with the peaks of the standard monoclinic $\text{R}_2\text{Ti}_2\text{O}_7$; whereas the spectra of Gd agree well with standard cubic $\text{R}_2\text{Ti}_2\text{O}_7$. The XRD and SEM of a cubic and monoclinic RET pyrochlore are shown in Figs. 2–6 to have an idea about their structure [30].

The SEM photographs show very fine sizes of the order of nanometer ranges for the powders. The $\text{La}_2\text{Ti}_2\text{O}_7$ (Fig. 3) and $\text{Nd}_2\text{Ti}_2\text{O}_7$ powders appear to be free in nature with fewer interconnections of the powder particles.

The SEM microstructure of the sintered (at 1450°C) monoclinic RETs exhibit a well sintered physical appearance for the broken cross-sectional structure of the discs. The grains are so smoothly interconnected with almost zero porosity and appear to be single domain in structure. The SEM microstructure of the cross-sectional surfaces of the $\text{La}_2\text{Ti}_2\text{O}_7$ discs sintered at 1450°C is given in Fig. 4.

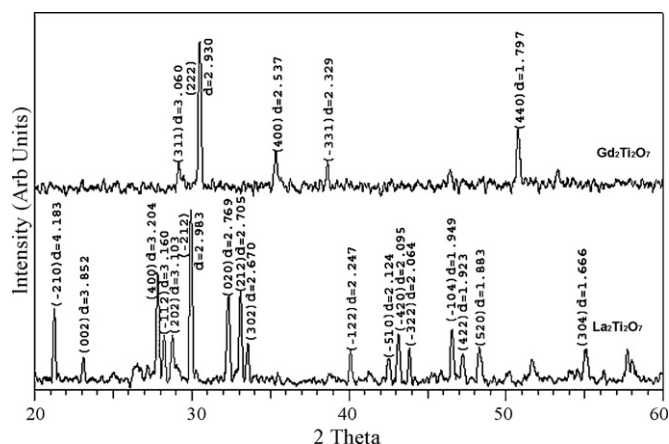


Fig. 2. Typical XRD spectra of $\text{Gd}_2\text{Ti}_2\text{O}_7$ (match JCPDS-ICDD 23-0259 cubic $\text{Gd}_2\text{Ti}_2\text{O}_7$) and $\text{La}_2\text{Ti}_2\text{O}_7$ (match JCPDS-ICDD 28-0517 monoclinic $\text{La}_2\text{Ti}_2\text{O}_7$) synthesized by SHS-urea method and calcined at 1200°C .

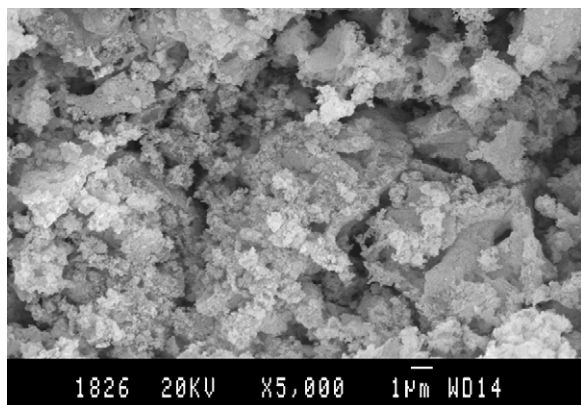


Fig. 3. SEM microstructure of SHS powders of monoclinic $\text{La}_2\text{Ti}_2\text{O}_7$.

The SEM of $\text{Gd}_2\text{Ti}_2\text{O}_7$ in Fig. 5 shows loosely packed powders along with some particles in a free state. SEM of cross-section of the sintered $\text{Gd}_2\text{Ti}_2\text{O}_7$ (1450 °C) discs made from SHS powders of cubic crystalline RETs is shown in Fig. 6. A comparison with SEM structure of sintered monoclinic titanates reveals that the cubic form is not well sintered even at temperatures of 1450–1500 °C, unlike the monoclinic material.

Fluorescence spectra due to the presence of RE ions in solids give information about the crystal field exerted on the respective elements in the compounds. The characteristic fluorescence spectra of different RE ions arise from the electronic transitions in the partially filled 4f orbitals. Electrons present in the occupied 4f shells can be transferred by light absorption, into unoccupied levels of

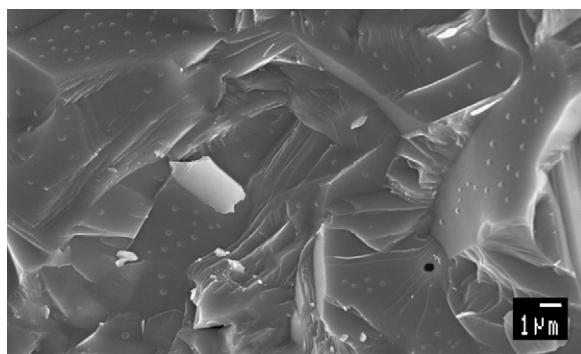


Fig. 4. SEM of the cross-section of sintered discs (at 1450 °C) of monoclinic $\text{La}_2\text{Ti}_2\text{O}_7$ made from SHS powders.

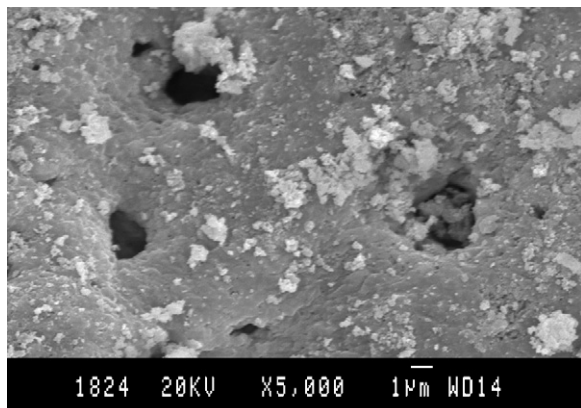


Fig. 5. SEM microstructure of SHS powders of cubic $\text{Gd}_2\text{Ti}_2\text{O}_7$.

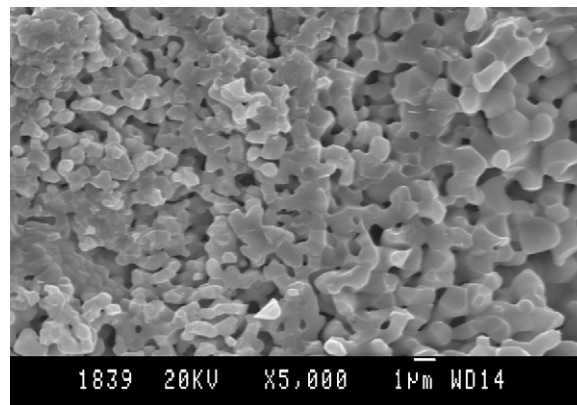


Fig. 6. SEM of the cross-section of sintered discs (at 1450 °C) of cubic $\text{Gd}_2\text{Ti}_2\text{O}_7$ made from SHS powders.

higher energies. The 4f orbitals are well shielded by the fully filled or partially filled 5s and 5p outer shells. As a result, emission lines are relatively narrow and the energy level structure varies only slightly from one host to another. The effect of the crystal field is normally treated as a perturbation on the free-ion levels. The perturbation is small compared to spin-orbit and electrostatic interactions among the 4f electrons. Since the splittings are small, the terms and their levels remain easily identifiable for the REs. The primary change in the energy levels due to a splitting of the free ion levels is caused by the Stark effect of the crystal field. In crystals the free-ion levels are then referred to as manifolds. The trivalent lanthanide ions show efficient extrinsic localized type luminescence of the characteristic line spectra owing to $f \leftarrow f$ forbidden type transition in the visible to near-infrared region. When atoms and ions are incorporated in crystals, the forbidden character of the electric dipole transition is altered by the perturbation of the crystal electric field, so that the forbidden transition becomes allowed to some degree [31]. Energy transfer from a light gathering meso-structured host lattice to an appropriate RE ion generates selected PL in the region 600–1540 nm. Exciting the titania in its band gap results in the energy transfer and it is possible to observe PL from the crystal field states of the RE ions [32].

The luminescence spectra recorded at a pump power of 100 mW using the CCD spectrograph assembly are shown in Fig. 7. The excited ions of the $\text{La}_2\text{Ti}_2\text{O}_7$ sample are observed to fluoresce with

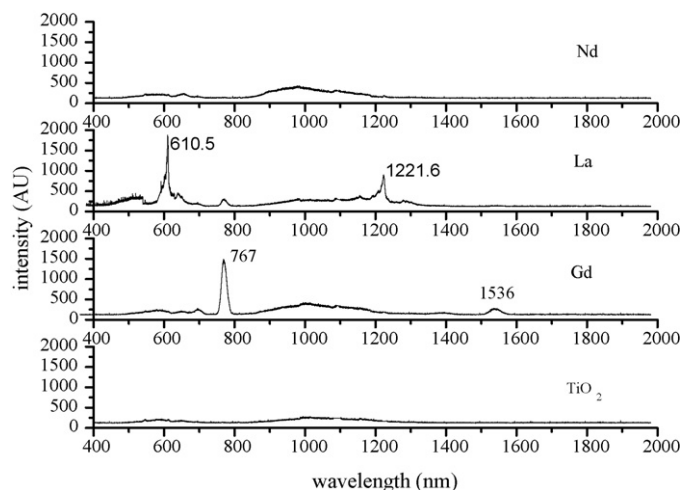


Fig. 7. Luminescence spectrum of the rare earth titanates when excited using 100 mW laser pulse of 355 nm.

peak emission within the range 608–612 nm region and also at 1221 nm which is the next harmonic. The spectrum of the TiO_2 is also given for comparison. The $\text{La}_2\text{Ti}_2\text{O}_7$ is reported to have direct band gap and act as a good photo-catalyst for different light absorption known for this kind of materials [2,8]. $\text{La}_2\text{Ti}_2\text{O}_7$ has a monoclinic structure with a space group of $\text{P}2_1$ at room temperature. Compounds with the pyrochlore structure have the formula $\text{A}_2\text{B}_2\text{B}'_2\text{O}_7$, where A can be the RE cation and B is Ti or any transition metal ions [33]. La^{3+} ion has a $[\text{Xe}] 4f^0$ inert gas configuration leading to a $^1\text{S}_0$ ground state. Excited states can arise from a p–d transition leading to the electronic configuration $5s^2 5p^5 5d^1$ which gives rise to the singlet $^1\text{P}_1$, $^1\text{D}_2$ and $^1\text{F}_3$ and the triplet $^3\text{P}_1$, $^3\text{D}_2$ and $^3\text{F}_3$ states [34]. Gd^{3+} has a $4f^7$ configuration and a ground state of $^8\text{S}_{7/2}$ [7,35–37].

The $\text{Gd}_2\text{Ti}_2\text{O}_7$ has peaks at 767 and 1536 nm. The second peak is observed to be the multiple of the first and hence can be considered as the harmonic. The $^6\text{I}_J$ to $^6\text{G}_J$ transitions give rise to the 767 nm emission from the Gd^{3+} ions. A broad spectrum near 1000 nm is also seen, which is produced by the TiO_6 octahedra centre that is common in all the RETs used for the present study. In the case of $\text{Nd}_2\text{Ti}_2\text{O}_7$ the spectrum is more prominent in this region (1000 nm) and can be associated with the emission due to the Nd^{3+} ions arising from $^4\text{F}_{3/2}$ to the $^4\text{I}_J$ ($^4\text{I}_{9/2}$: 900 nm, $^4\text{I}_{11/2}$: 1060 nm, $^4\text{I}_{13/2}$: 1350 nm) transitions.

It has been reported earlier that the transition metal activator Ti^{3+} ions in insulating laser crystals have spectral stimulated emission (SE) near 611 nm and within the range 660–1180 nm with the SE channel $^2\text{E} \rightarrow ^2\text{T}_2$ for operating temperature 300 K and at laser pumping conditions [38]. Ions with no 4f electrons are reported to have no electronic energy levels that can induce excitation and luminescence processes in or near the visible region [31]. However, in the case of $\text{La}_2\text{Ti}_2\text{O}_7$ a transition close to 611 nm is observed in our studies. The luminescent peaks observed at 610 and 1221 nm are sharp and it can be credited to the unfilled 4f orbital of the RE (La) added. An enhancement in the emission at around 610 nm is due to the presence of the unfilled 4f orbital of the La^{3+} ions present in the TiO_6 octahedra centres. Transition of the La^{3+} from the excited $^3\text{F}_4$ state to the ground state $^1\text{S}_0$ enhances the Ti^{3+} SE channel near 611 nm to give rise to the luminescence at 610 nm for the $\text{La}_2\text{Ti}_2\text{O}_7$. The La^{3+} with the unfilled 4f orbital acts as a sensitizer and enhances the SE of the Ti^{3+} . The crystal field splitting can also be observed in the resolved spectrum which is shown in Fig. 8. Internal 4f transitions are observed at wavelengths shorter

than the absorption edges. There is no contribution from the La to the valence band [2]. The various Russell–Saunders states arising from the $4f^n$ configurations are split by the crystal field, but the splitting is about 100 cm^{-1} . The extremely small splitting makes the f–f absorption bands very sharp giving rise to line-like spectra.

The R 4f level in $\text{R}_2\text{Ti}_2\text{O}_7$ is shifted to lower energy as the number of R 4f electrons increases. This red shift of the R 4f band decreases the band gap energy of the $\text{R}_2\text{Ti}_2\text{O}_7$ [2]. Thus a red shift in the luminescence to Gd^{3+} ions with respect to La^{3+} ions is also observed as the R^{3+} ion radius is decreased due to lanthanide contraction. This explains the red shift exhibited by Gd^{3+} ions which has a smaller ionic radius with respect to La^{3+} ions.

The observed luminescence property may be attributed to La^{3+} centre in the nano-sized $\text{La}_2\text{Ti}_2\text{O}_7$ whereas for the other titanates it may be attributed to TiO_6 octahedra centres. Thus nano-sized $\text{La}_2\text{Ti}_2\text{O}_7$ is a promising red phosphor for display applications.

5. Conclusions

The luminescence shown by the nano-sized $\text{La}_2\text{Ti}_2\text{O}_7$ in the visible region is due to the presence of the unfilled 4f orbital of the La^{3+} ions in the TiO_6 octahedra centres even though ions with no 4f electrons do not have such emission in this region. The SE of transition metal activator Ti^{3+} ions in insulating laser crystals near 611 nm can be enhanced by the sensitizer La^{3+} ions and it is sharp due to the presence of the 4f orbitals. In other RETs, this SE is inhibited by the presence of R^{3+} ions in 4f orbital. In the case of $\text{Nd}_2\text{Ti}_2\text{O}_7$ the fluorescence emission of the Nd^{3+} ions is overlapped by the presence of the Ti^{3+} SE channels. A red shift in the luminescence of Gd^{3+} ions with respect to La^{3+} ions is observed as the R^{3+} ion radius is decreased due to lanthanide contraction. The observed luminescence of nano-sized $\text{La}_2\text{Ti}_2\text{O}_7$ near 610 nm makes it suitable for display applications after further characterizations.

Acknowledgment

The author LKJ is thankful to UGC (Govt. of India) for financial support.

References

- [1] I. Burn, S. Neirman, *J. Mater. Sci.* 17 (1982) 3510.
- [2] D.W. Hwang, J.S. Lee, W. Li, S.H. Oh, *J. Phys. Chem. B* 107 (2003) 4963.
- [3] M.A. Subramanian, G. Aravamudan, G.V. Subba Rao, *Prog. Solid State Chem.* 15 (2) (1983) 55.
- [4] K.B. Helean, S.V. Ushakov, C.E. Brown, A. Navrotsky, J. Lian, R.C. Ewing, J.M. Farmer, L.A. Boatner, *J. Solid State Chem.* 177 (6) (2004) 1858.
- [5] F.X. Zhang, S.K. Saxena, *Chem. Phys. Lett.* 413 (1–3) (2005) 248.
- [6] N. Zhong, P.-H. Xiang, D.-Z. Sun, X.-L. Dong, *Mater. Sci. Eng. B* 116 (2) (2005) 140.
- [7] S.T. Bramwell, M.N. Field, M.J. Harris, I.P. Parkin, *J. Phys. Condens. Matter* 12 (2000) 483.
- [8] R. Abe, M. Higashi, K. Sayama, Y. Abe, H. Sugihara, *J. Phys. Chem. B* 110 (2006) 2219.
- [9] K.E. Sickafus, L. Minervini, R.W. Grimes, J.A. Valdez, M. Ishimaru, F. Li, K.J. McClellan, T. Hartmann, *Science* 289 (2000) 748.
- [10] J. Wu, X. Wei, N.P. Padture, P.G. Klemens, M. Gell, E. Garcia, P. Miranzo, M.I. Osendi, *Cheminform* 34 (10) (2003), doi:10.1002/chin.200310007.
- [11] Ewing F.R.C., W.J. Weber, Lian S.J., *J. Appl. Phys.* 95 (11) (2004) 5949.
- [12] Y. Teraoka, K.-I. Torigoshi, H. Yamaguchi, T. Ikeda, S. Kagawa, *J. Mol. Catal. A: Chem.* 155 (1/2) (2000) 73.
- [13] H. Lehmann, D. Pitzer, G. Pracht, R. Vassen, D. Stover, *J. Am. Ceram. Soc.* 86 (8) (2003) 1338.
- [14] J. Shi, J. Chen, Z. Feng, T. Chen, Y. Lian, X. Wang, C. Li, *J. Phys. Chem. C* 111 (2007) 693.
- [15] H. Yamamoto, S. Okamoto, H. Kobayashi, *J. Lumin.* 100 (1–4) (2002) 325.
- [16] S. Okamoto, H. Yamamoto, *J. Lumin.* 102/103 (2003) 586.
- [17] J.C. Krupa, in: B.N. Jagatap, A. Venugopalan (Eds.), *Recent Developments in Spectroscopy of Lanthanides and Actinides*, R V Enterprises, Mumbai, 2006, p. 41.
- [18] M. Morita, S. Buddhudu, D. Rau, S. Murakami, *Optical spectra and chemical bonding in transition metal complexes* 'Photoluminescence and excitation

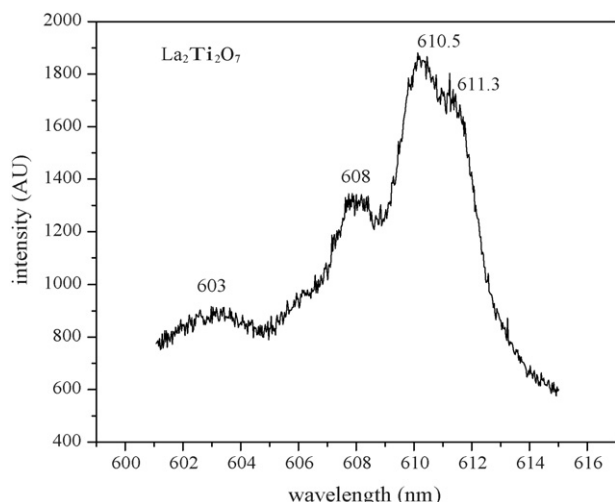


Fig. 8. Crystal field splitting shown by $\text{La}_2\text{Ti}_2\text{O}_7$.

- energy transfer of rare earth ions in nanoporous xerogel and sol-gel SiO₂ glasses' (Berlin: Springer), Struct. Bond 104 (2004) 115.
- [19] S. Buddhudhu, M. Morita, S. Murakami, D. Rau, J. Lumin. 83/84 (1999) 199.
- [20] M. Morita, D. Rau, S. Kajiyama, T. Sakurai, M. Baba, M. Iwamura, Mater. Sci. Poland 22 (1) (2004) 5.
- [21] Y. Zhang, H. Zhang, Y. Xu, Y. Wang, J. Mater. Chem. 13 (2003) 2261.
- [22] Z. Xu, Q. Yang, C. Xie, W. Yan, Y. Du, Z. Gao, J. Zhang, J. Mater. Sci. 40 (6) (2005) 1539.
- [23] J.-H. Park, M.-G. Kwak, C.S. Kim, D.-H. Yoo, H.-S. Yang, B.K. Moon, B.-C. Choi, H.J. Seo, E.D. Jeong, K.S. Hong, J. Korean Phys. Soc. 48 (6) (2006) 1369.
- [24] J.-H. Park, N.G. Back, K.-S. Hong, C.-S. Kim, D.-H. Yoo, M.G. Kwak, J.-I. Han, J.-H. Sung, B.K. Moon, H.-J. Seo, B.-C. Choi, J. Korean Phys. Soc. 47 (2005) S368.
- [25] V. Hlavacek, Am. Ceram. Soc. Bull. 70 (2) (1991) 240.
- [26] H.C. Yi, J.J. Moore, J. Mater. Sci. 25 (2) (1990) 1159.
- [27] Z.A. Munir, U. Anselmi-Tamburini, Mater. Sci. Rep. 3 (7/8) (1989) 277.
- [28] A.G. Merzhanov, J. Mater. Chem. 14 (2004) 1779.
- [29] K.C. Patil, S.T. Aruna, S. Ekambaram, Curr. Opin. Solid State Mater. Sci. 2 (2) (1997) 158.
- [30] K.R. Dayas, Self propagated high temperature synthesis of electroceramic rare earth titanates and its characterization, Ph.D. Thesis, Calicut University, Calicut, India, 2006.
- [31] S. Shionoya, in: D.R. Vij (Ed.), Luminescence of Solids, Plenum Press, New York, 1998, p. 95.
- [32] K.L. Frindell, M.H. Bartl, M.R. Robinson, G.C. Bazan, A. Popitsch, G.D. Stucky, J. Solid State. Chem. 172 (1) (2003) 81.
- [33] A.W. Sleight, Inorg. Chem. 8 (1969) 1807.
- [34] R.H. Abu-Eittah, S.A. Marie, M.B. Salem, Can. J. Anal. Sci. Spectrosc. 49 (4) (2004) 248.
- [35] S.N. Datta, in: B.N. Jagatap, A. Venugopalan (Eds.), Recent Developments in Spectroscopy of Lanthanides and Actinides, R V Enterprises, Mumbai, 2006, p. 17.
- [36] G.H. Dieke, H.M. Crosswhite, Appl. Opt. 2 (7) (1963) 675.
- [37] W. Koechner, M. Bass, Solid State Lasers, Springer, New York, 2003.
- [38] A.A. Kaminskii, Crystalline Lasers: Physical Processes and Operating Schemes, CRC Press, USA, 1996, Chapter 1.